Electronic Supplementary Material (ESI) for ChemComm.

Electronic Supplementary Information

The Photothermal Effect in MOFs: Covalent Post-Synthetic Modification of MOFs Mediated by UV-Vis Light under Solvent-Free Conditions†

Jordi Espín,[a] Luis Garzón-Tovar,[a] Gerard Boix,[a] Inhar Imaz[a] and Daniel Maspoch*[ab]

[a]Catalan Institute of Nanoscience and Nanotechnology (ICN2), CSIC and The Barcelona Institute of Science and Technology, Campus UAB, Bellaterra, 08193 Barcelona, Spain

[b]ICREA, Pg. Lluís Companys 23, 08010 Barcelona, Spain

Section S1: Materials, instrumentation and synthetic procedures

1. Materials and instrumentation

Reagents were purchased from Sigma Aldrich and from Fisher Scientific, respectively, and used without further purification. Deionised water was obtained with a Milli-Q system (18.2 MΩ cm). X-Ray Powder Diffraction (XRPD) patterns were collected on an X'Pert PRO MPDP analytical diffractometer (Panalytical) at 45 kV and 40 mA with CuKα radiation ($\lambda = 1.5419$ Å). Nitrogen adsorption measurements were done at 77 K with an Autosorb-IQ-AG analyser (Quantachrome Instruments). The ^{1}H-NMR spectra of digested UiO-66-NH$_2$ and MIL-101-NH$_2$-(Al) were collected on a 400MHz Bruker AVANCE III spectrometer. A Bluepoint 4 Ecocure (Hönle UV Technology), high-intensity, UV-Vis high-intensity spot lamp without filter (300 nm - 650 nm) and a PI 450 (Optris) infrared camera, working in a temperature range of 0 - 250 °C, was used. Data were obtained using the PI Connect software.

2. Experimental set-ups used for MOF activation and for Covalent Post-Synthetic Modification (CPSM) of MOFs

Activation:

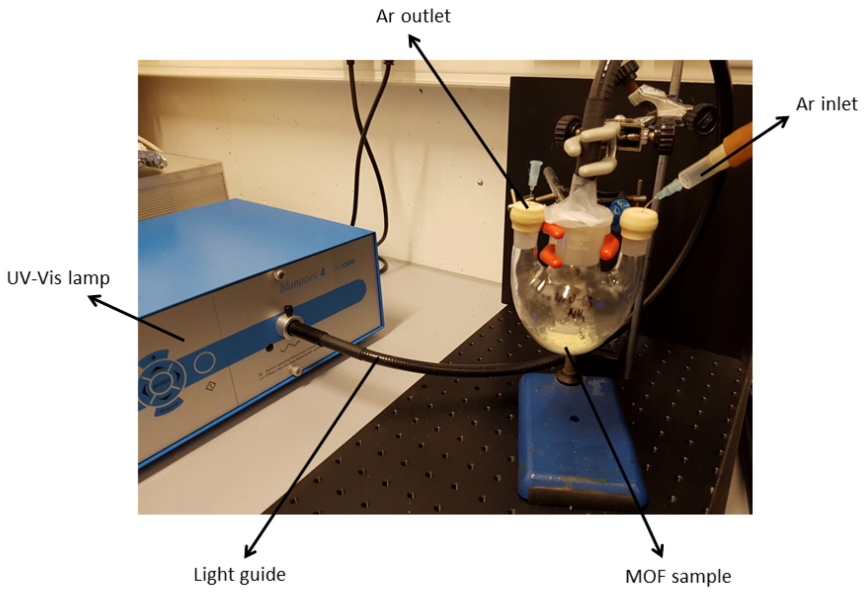

The sample was placed in a three-neck round-bottom flask and the light guide was set at the desired distance. Argon flow was applied using an inlet needle through a septum, and was then purged through an outlet. The light guide neck was capped with Parafilm. The entire set-up was covered to protect it from light, and then the sample was irradiated for a certain period of time.

CPSM:

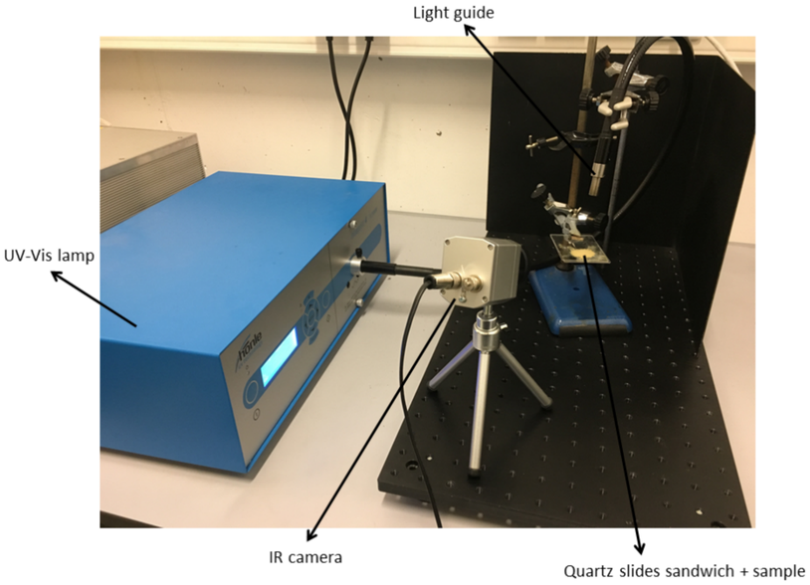

The solid mixture was placed between two quartz slides, forming a round pellet, and the light guide was set at the desired distance from the slide “sandwich”. The sample was then irradiated (UV-Vis light: 300 nm - 650 nm) for a certain period of time.

3. Synthetic procedures

3.1 Synthesis of UiO-66-NH_2.

UiO-66-NH_2 was synthesised following a previously reported method [F. Ragon, P. Horcajada, H. Chevreau, Y. K. Hwang, U. H. Lee, S. R. Miller, T. Devic, J.-S. Chang and C. Serre, *Inorg. Chem.*, 2014, **53**, 2491-250]. In a typical synthesis, 16.1 g (0.05 mol) of $ZrOCl_2 \cdot 8H_2O$ was dissolved in 125 mL of DMF at room temperature under stirring for 15 min. In a separate flask, NH_2-bdc (8.3 g, 0.05 mol) was dissolved in 125 mL of DMF at room temperature under stirring for 15 min. The yellow NH_2-bdc solution obtained was added to the $ZrOCl_2 \cdot 8H_2O$ solution, followed by addition of 3 mL of HCl 37% under stirring. The resulting mixture was heated at 120 °C under stirring for 4 h. The obtained solid was collected by centrifugation at 9000 rpm for 5 min, washed two times with 100 mL of DMF for 12 h and two times with 100 mL of absolute ethanol for 12 h. Finally, the resulting powder was dried at 85 °C overnight.

3.2 Synthesis of MIL-101-NH_2-(Al).

MIL-101-NH_2-(Al) was synthesised following a previously reported method [H. Hintz and S. Wuttke, *Chem. Mater.*, 2014, **26**, 6722-6728]. In a typical synthesis, 0.514 g (2.10 mmol) of aluminium chloride hexahydrate was dissolved in 15 mL of DMF. In a separate flask, 0.563 g (3.10 mmol) of NH_2-bdc was dissolved in 15 mL of DMF at room temperature. The yellow NH_2-bdc solution obtained was added to the $AlCl_3 \cdot 6H_2O$ solution under stirring. The resulting mixture was heated for 72 h at 130 °C in an oven. The resulting solid was collected by centrifugation at 9000 rpm for 5 min, washed absolute ethanol (2 x 200 mL) at 80 °C. Finally, the resulting powder was dried at 85 °C overnight.

3.3 UV-Vis CPSM procedure

In a typical CPSM experiment, 25 mg of MOF (UiO-66-NH_2 or MIL-101-NH_2-(Al)) and a pre-determined number of molar equivalents of the anhydride (relative to the amino group of the unit cell), were ground gently in a mortar for 5 min to create a homogeneous solid mixture. The sample was then spread between two quartz slides and the light guide was placed at a distance of 7 cm (500 $mW \cdot cm^{-2}$). Irradiation was applied during 15 min in each side of the quartz sandwich and the temperature was monitored using an IR camera. The resulting solid was washed with DMF (2 x 10 mL), soaked in DMF for 24 h, and then washed with acetone (4 x 10 mL). The washed material was digested in 120 µL of 5% HF in D_2O and 500 µL of d_6-DMSO for further ^{1}H-NMR analysis.

3.4 UV-Vis irradiation of each reagent

To demonstrate that photothermally activated MOFs act as “heaters” for CPSMs, 25 mg of each MOF alone were irradiated under the same conditions used above for the CPSM experiments (500 $mW \cdot cm^{-2}$ and 15 min/side). The maximum temperature attained in UiO-66-NH_2 was 78 °C and in MIL-101-NH_2-(Al), 72 °C. Contrariwise, as a control experiment to demonstrate that anhydrides cannot be photothermally activated, maleic anhydride and benzoic anhydrides were each irradiated alone under the same conditions. Maleic anhydride reached only 27 °C and benzoic anhydride, only 30 °C, thus confirming the lack of photothermal effect.

Section S2: Supplementary Figures

UiO-66-NH_2

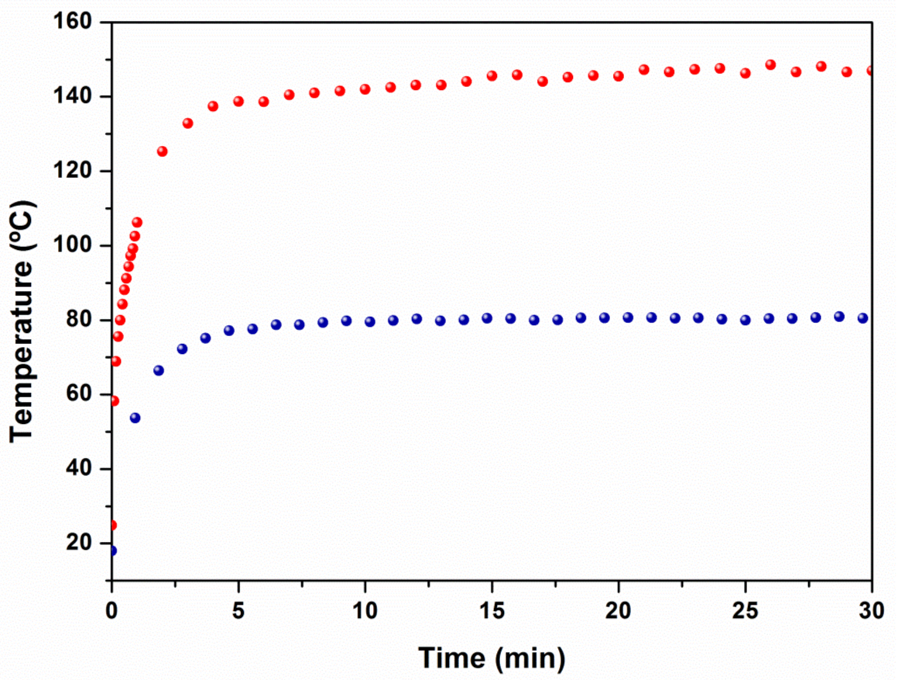

Figure S1. Change in temperature over time for 100 mg (red) and 25 mg (blue) of UiO-66-NH_2 irradiated at 500 mW·cm^{-2} (light guide-to-sample distance: 7 cm) for 30 min.

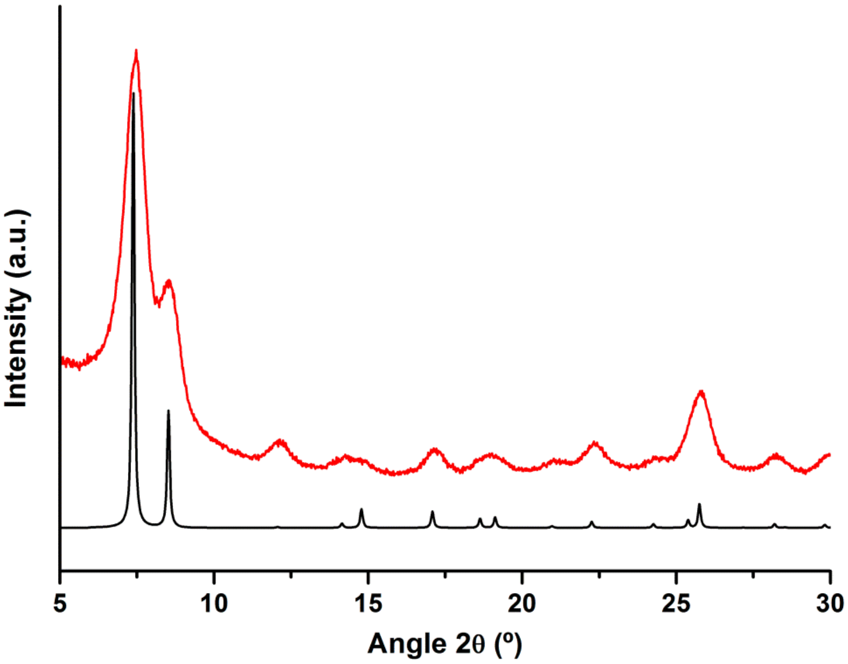

Figure S2. XRPD patterns for simulated UiO-66-NH_2 (black) and activated (red) UiO-66-NH_2.

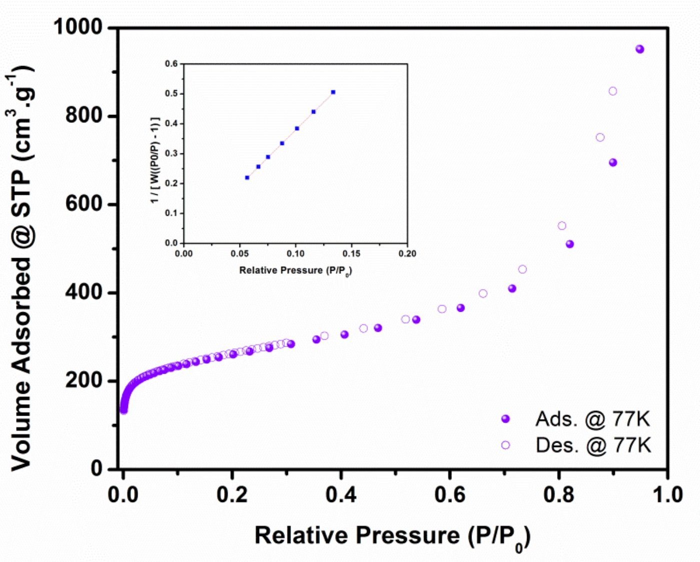

BET surface area: 935.732 m²/g

Slope: 3.713 g/cm^3 STP

Intercept: 8.964e-03 g/cm^3 STP

Correlation coefficient: 0.999983

C constant: 415.193

Molecular cross-sectional area: 0.1620 nm²

Figure S3. N_2 adsorption isotherm and BET linear fit for synthesised UiO-66-NH_2.

CPSM of UiO-66-NH_2 with maleic anhydride (MA)

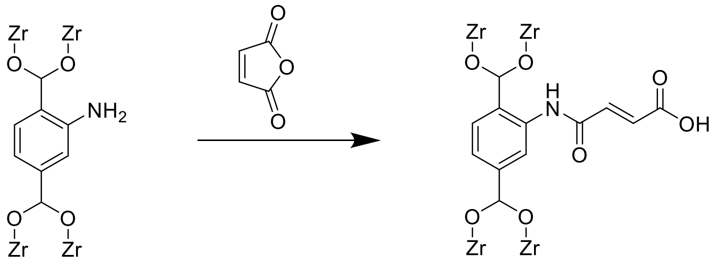

Before Irradiation	After Irradiation	Infrared camera image
	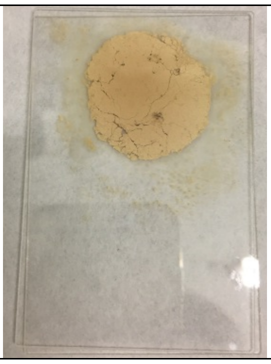	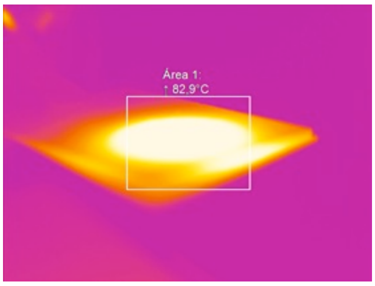

Figure S4. Photos of the formation of (UiO-66-MA)$_3$ upon UV-Vis irradiation (500 mW·cm^{-2}) of UiO-66-NH_2 and MA: before (left), after (middle) and infrared camera image during irradiation (right).

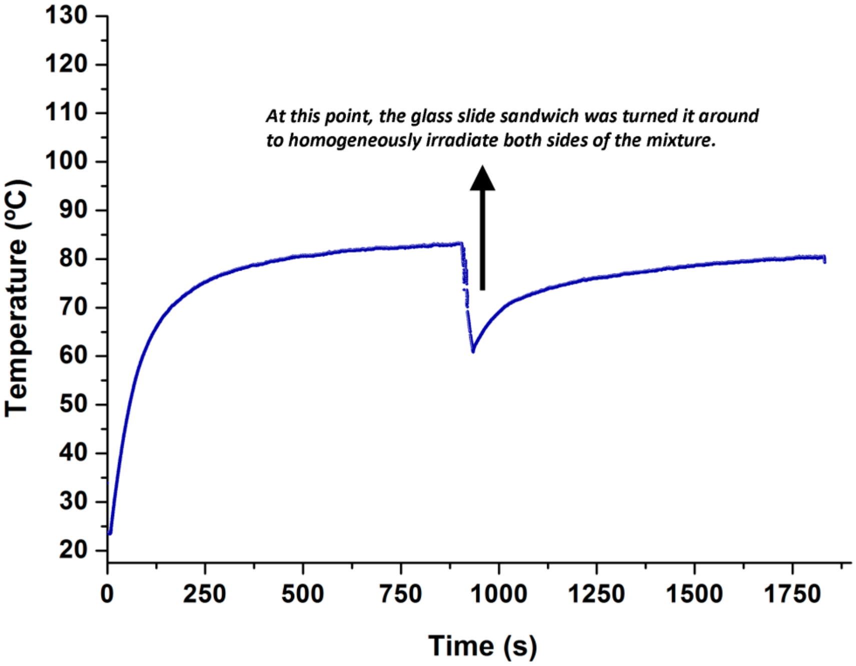

Figure S5. Photothermal plot of the formation of (UiO-66-MA)$_3$ upon UV-Vis irradiation of UiO-66-NH_2 and MA at 500 mW·cm^{-2}.

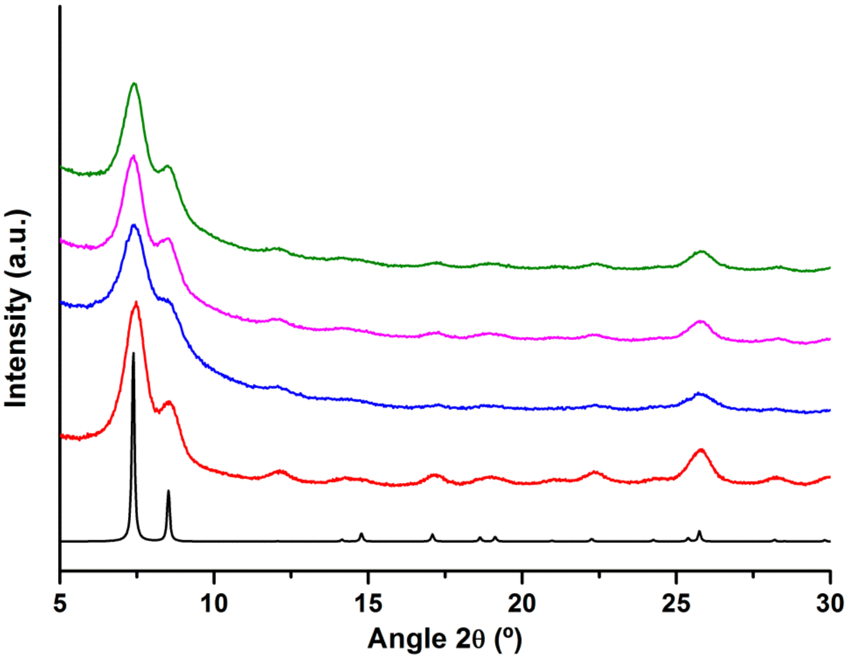

Figure S6. XRPD patterns for synthesised (UiO-66-MA)$_x$ (blue: x = 1; pink: x = 3; green: x = 6), activated UiO-66-NH$_2$ (red) and simulated UiO-66-NH$_2$ (black).

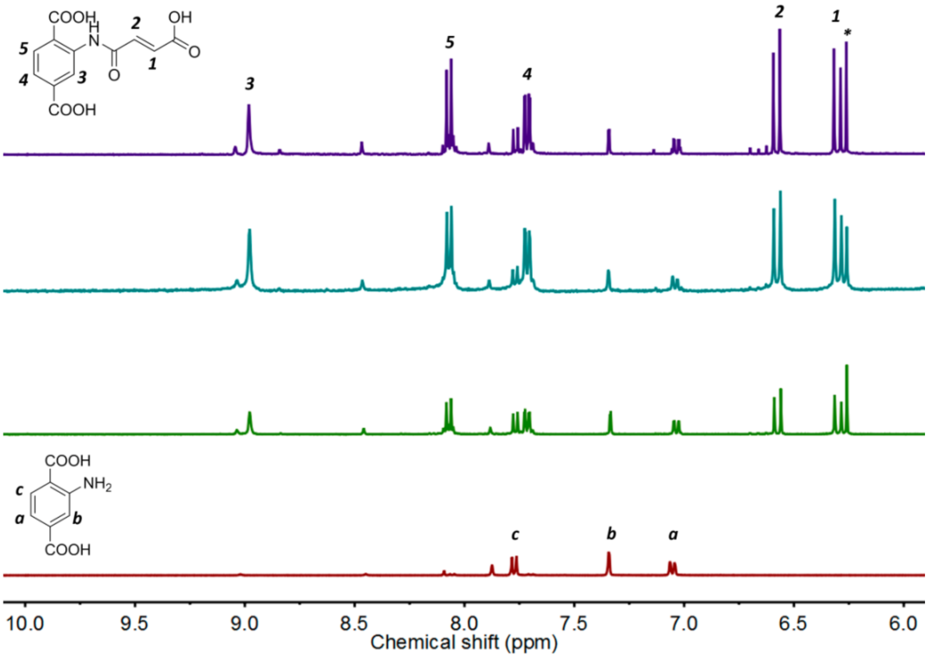

Figure S7. ^{1}H NMR spectra of digested (UiO-66-MA)$_x$ at molar ratios (NH$_2$/bdc:MA) of 1:1 (green; x = 1), 1:3 (blue; x = 3) or 1:6 (purple; x = 6), as compared to the spectrum of activated UiO-66-NH$_2$ (red). NMR solvent: DMSO-*d*$_6$/HF.

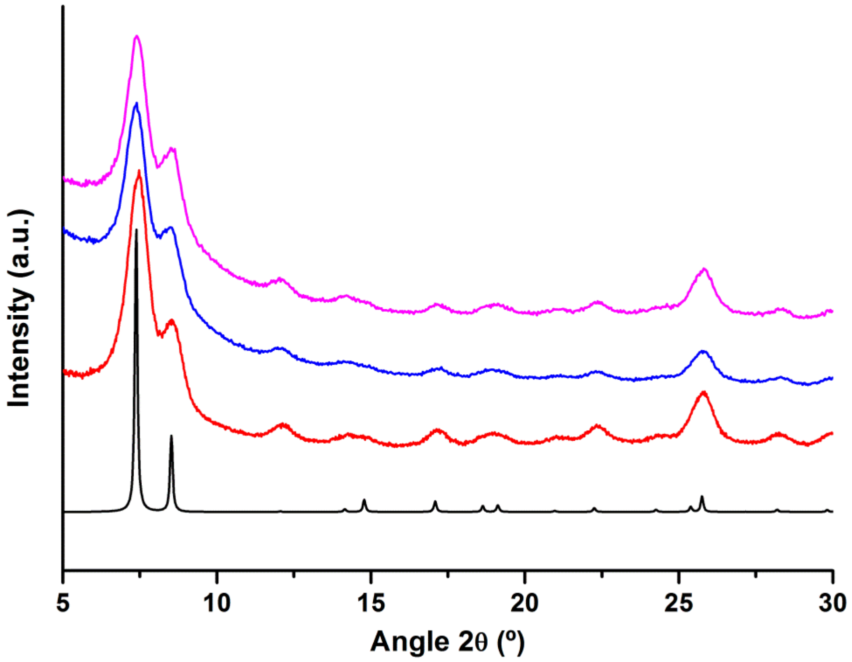

Figure S8. XRPD patterns for synthesised $(UiO\text{-}66\text{-}MA)_3$ irradiated at either 500 mW·cm^{-2} (blue) or 900 mW·cm^{-2} (pink), as compared to those for activated UiO-66-NH_2 (red) and simulated UiO-66-NH_2 (black).

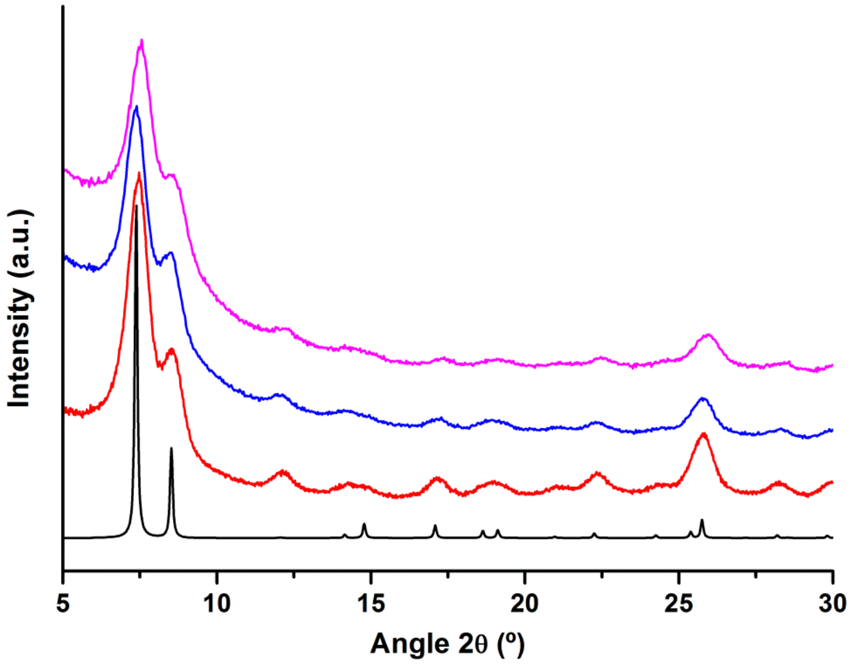

Figure S9. XRPD patterns for $(UiO\text{-}66\text{-}MA)_3$ irradiated for 30 min (blue) or 60 min (pink), as compared to those for activated UiO-66-NH_2 (red) and simulated UiO-66-NH_2 (black).

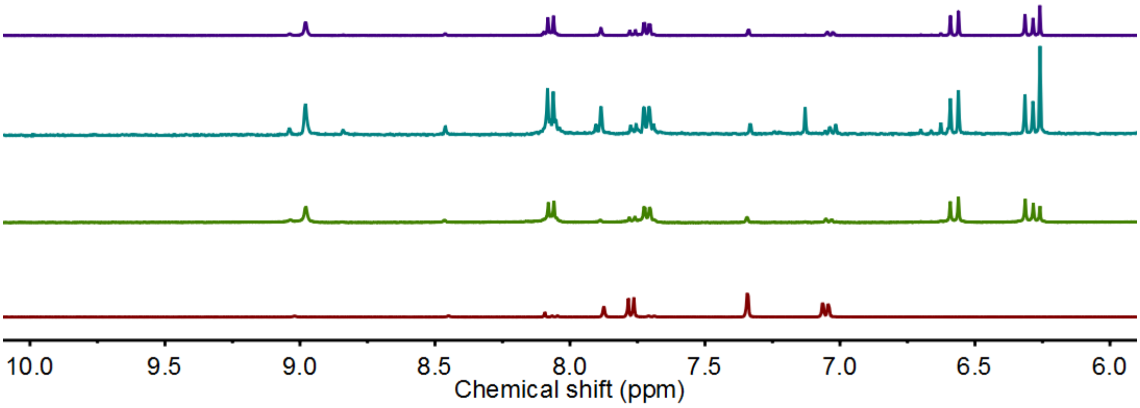

Figure S10. ^{1}H NMR spectra of digested (UiO-66-MA)$_3$, irradiated at either 500 mW·cm^{-2} (green) or 900 mW·cm^{-2} (blue) for 30 minutes, and irradiated at 500 mW·cm^{-2} for 60 minutes (purple), as compared to the spectrum of activated UiO-66-NH$_2$ (red). NMR solvent: DMSO-*d*$_6$/HF.

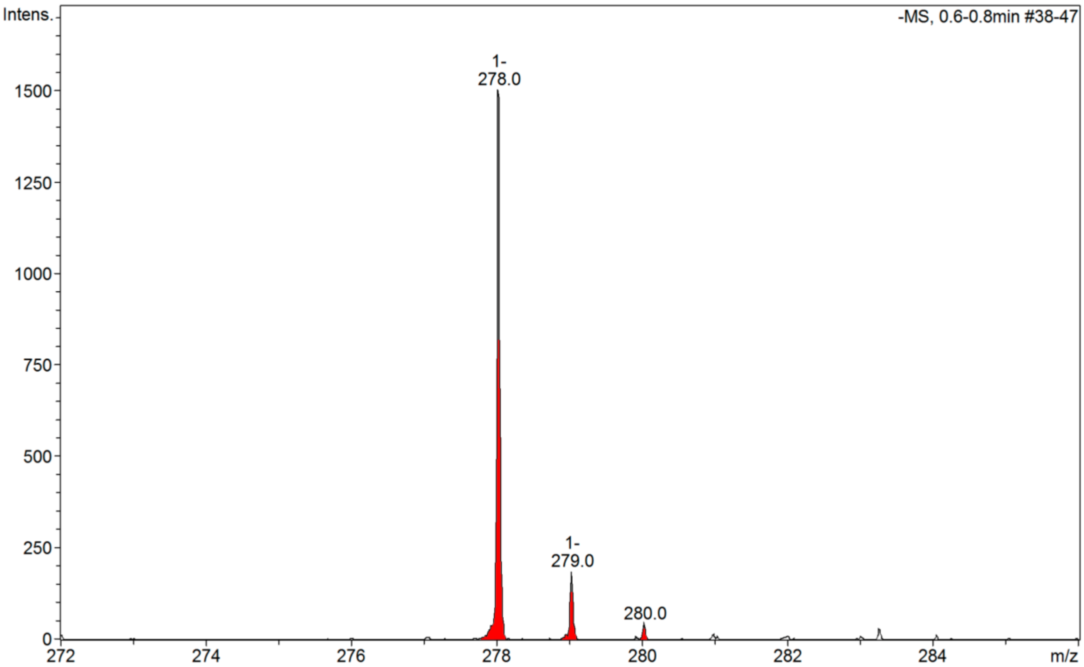

Figure S11. ESI-MS spectrum of digested (UiO-66-MA)$_3$.

CPSM of UiO-66-NH$_2$ with benzoic anhydride (BA)

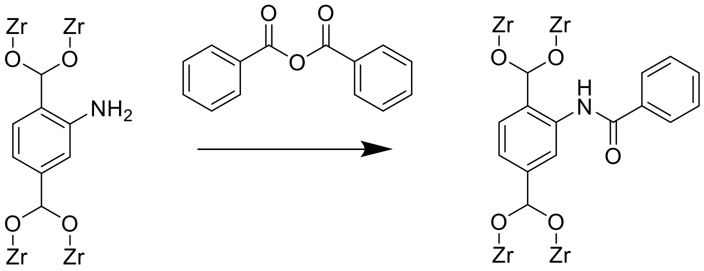

Before Irradiation	After Irradiation	Infrared camera image
		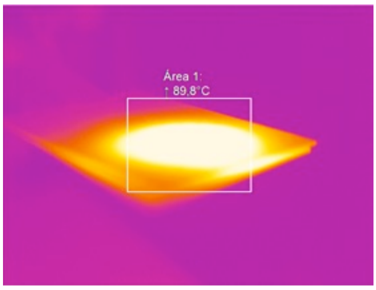

Figure S12. Photos of the formation of (UiO-66-BA)$_3$ upon UV-Vis irradiation (500 mW·cm^{-2}) of UiO-66-NH$_2$ and BA: before (left), after (middle) and infrared camera image during irradiation (right).

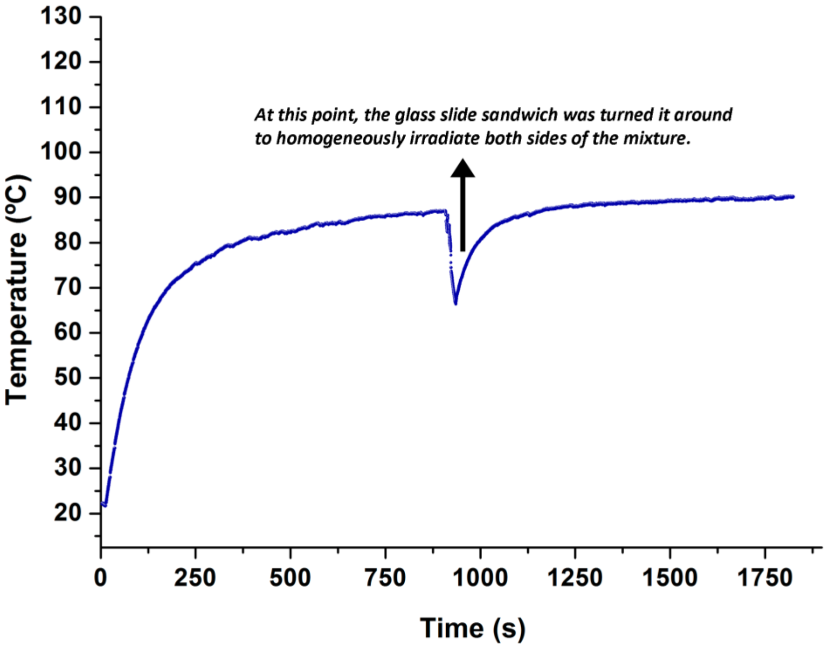

At this point, the glass slide sandwich was turned it around to homogeneously irradiate both sides of the mixture.

Figure S13. Photothermal plot of the formation of (UiO-66-BA)$_3$ upon UV-Vis irradiation of UiO-66-NH$_2$ and BA at 500 mW·cm^{-2}.

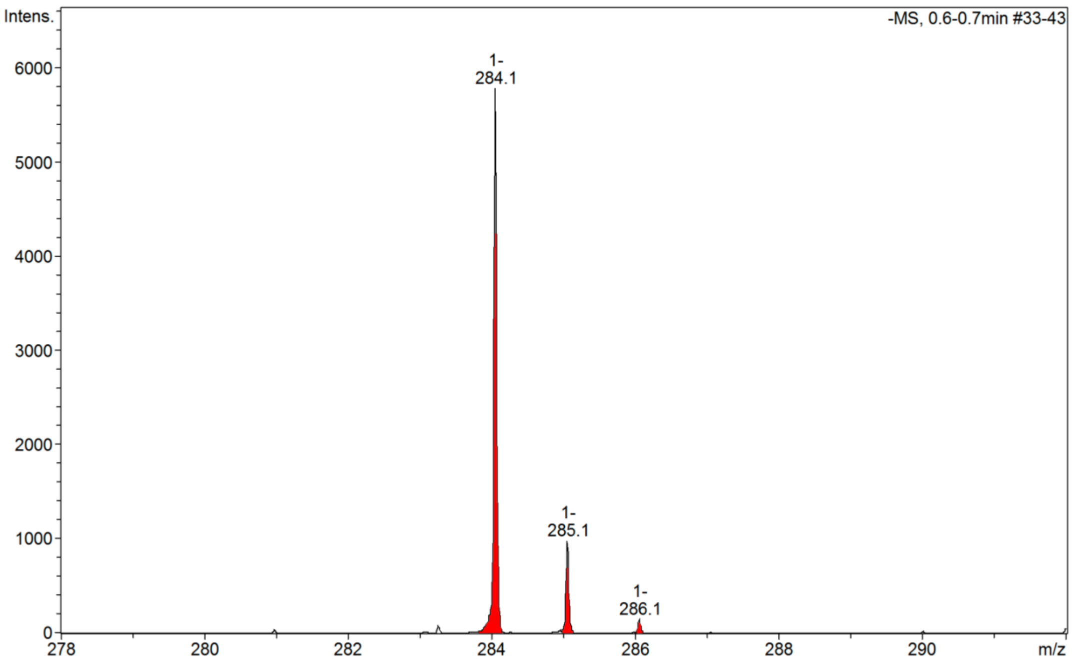

Figure S14. ESI-MS spectrum of digested $(UiO\text{-}66\text{-}BA)_3$.

MIL-101-NH$_2$-(Al)

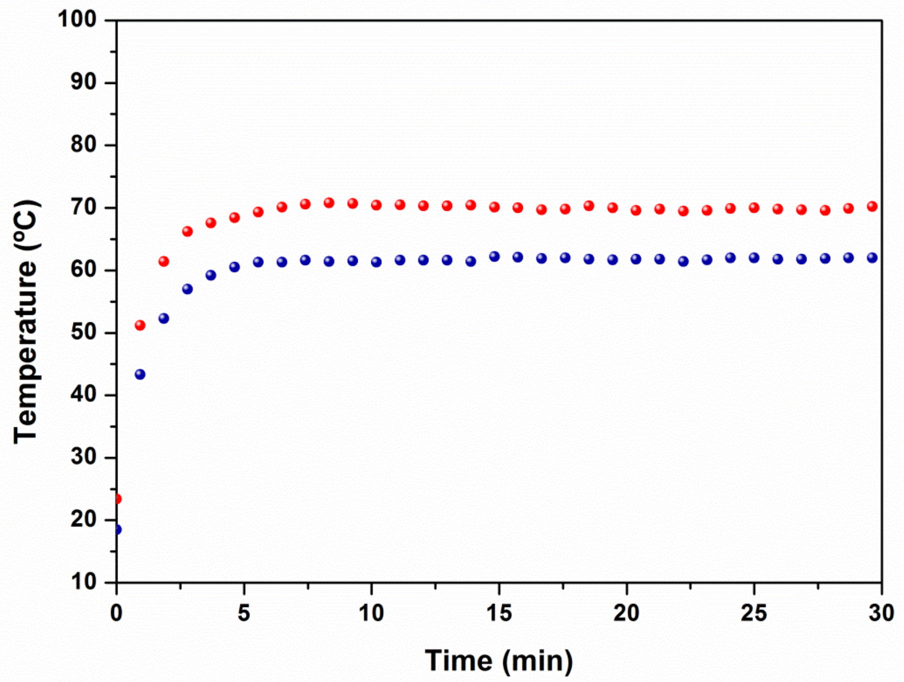

Figure S15. Photothermal plots of the irradiation of MIL-101-NH$_2$-(Al) (25 mg) at 265 mW·cm^{-2} (blue) or 500 mW·cm^{-2} (red).

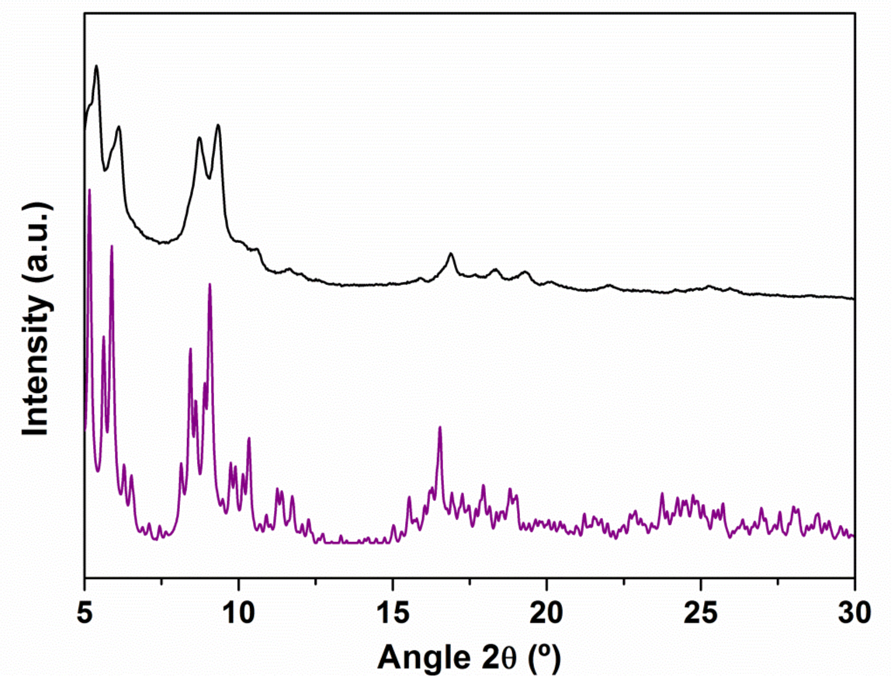

Figure S16. XRPD patterns for simulated MIL-101-NH$_2$-(Al) (purple) and synthesised MIL-101-NH$_2$-(Al) (black).

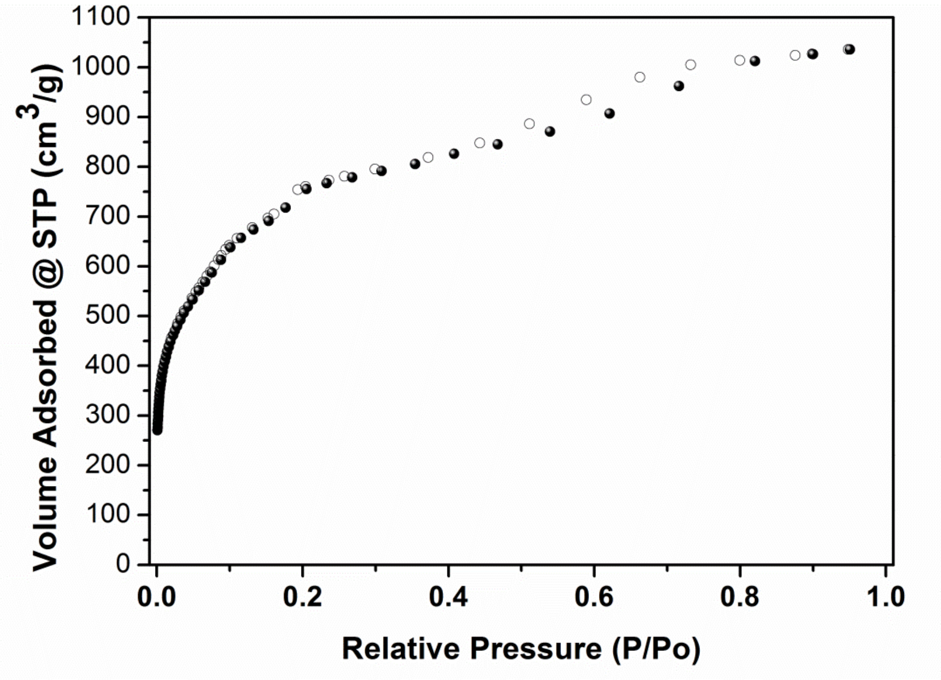

Figure S17. N_2 adsorption isotherm for synthesised MIL-101-NH_2-(Al).

CPSM of MIL-101-NH_2-(Al) with maleic anhydride (MA)

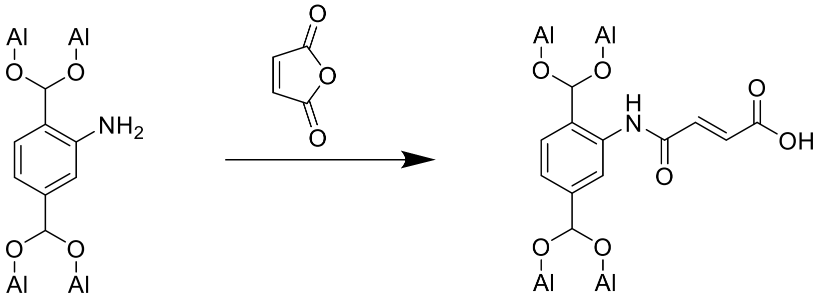

Before Irradiation	After Irradiation	Infrared camera image
		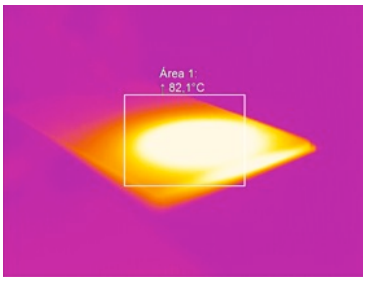

Figure S18. Photos of the formation of (MIL-101-(Al)-MA)$_3$ upon UV-Vis irradiation (500 mW·cm^{-2}) of MIL-101-NH_2-(Al) and MA: before (left), after (middle) and infrared camera image during irradiation (right).

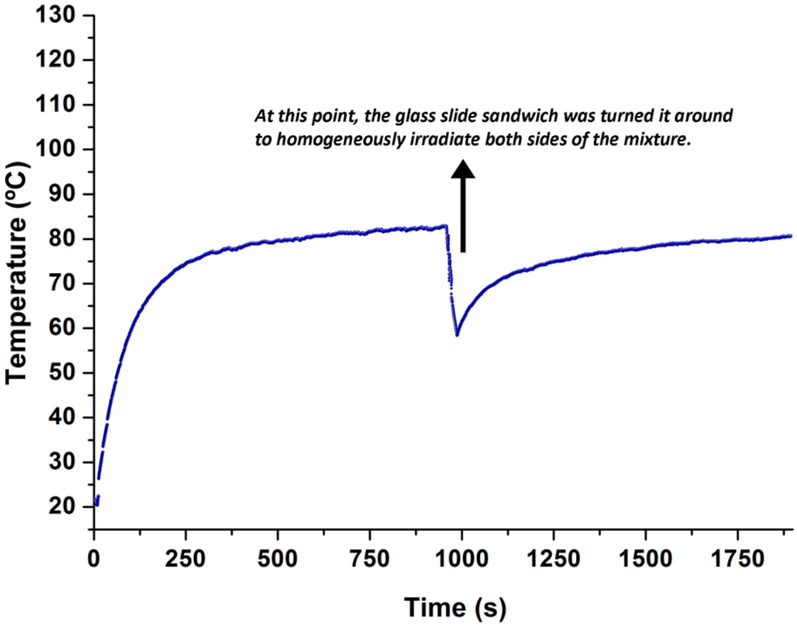
At this point, the glass slide sandwich was turned it around to homogeneously irradiate both sides of the mixture.

Figure S19. Photothermal plot of the formation of (MIL-101-(Al)-MA)$_3$ upon UV-Vis irradiation of MIL-101-NH_2-(Al) and MA at 500 mW·cm^{-2}.

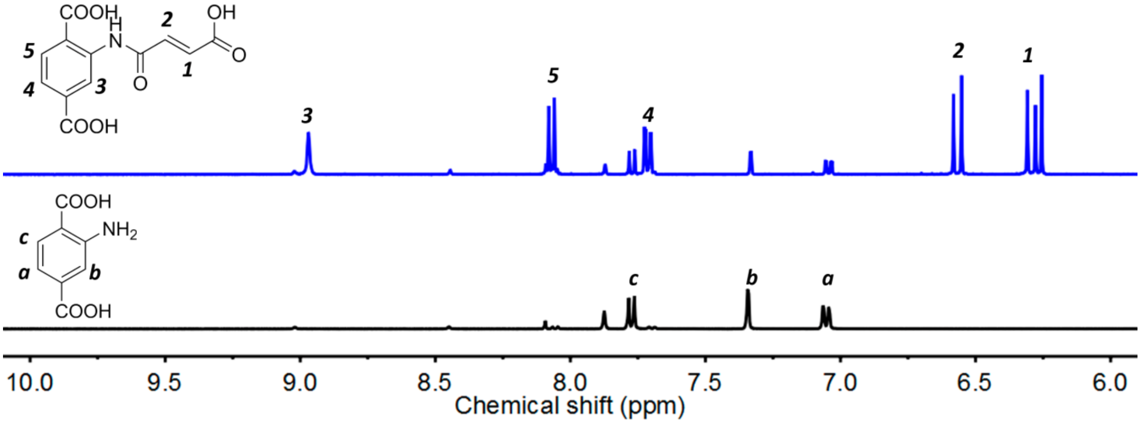

Figure S20. ^{1}H NMR spectrum of digested (MIL-101-(Al)-MA)$_3$ (blue), as compared to that of activated MIL-101-NH$_2$-(Al) (black). NMR solvent: DMSO-d_6/HF.

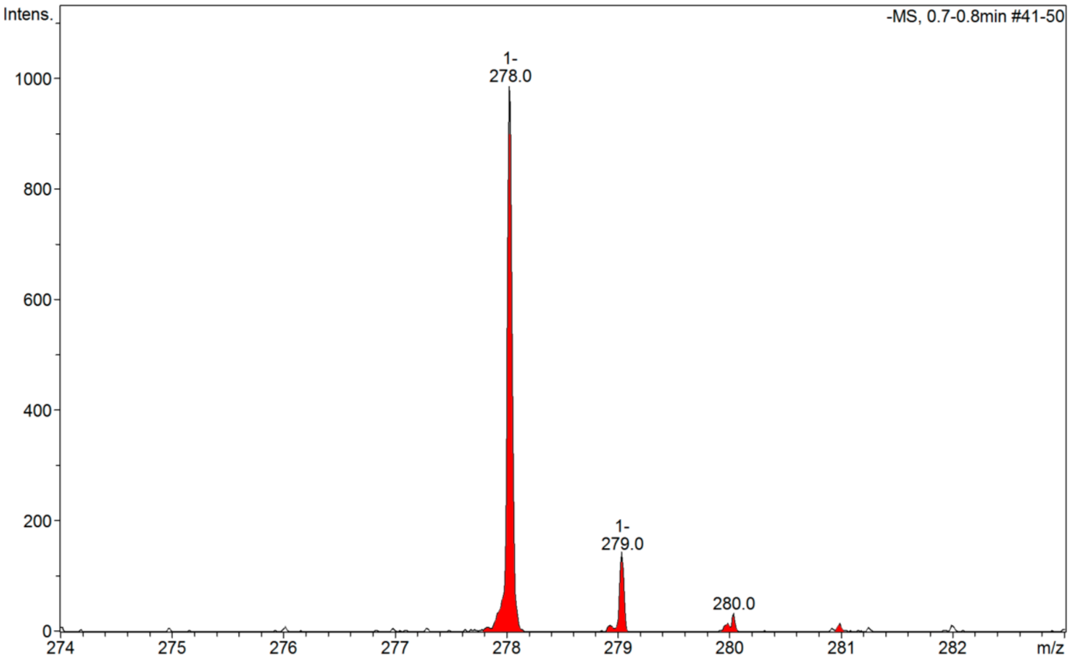

Figure S21. ESI-MS spectrum of digested (MIL-101-(Al)-MA)$_3$

CPSM of MIL-101-NH_2-(Al) with benzoic anhydride (BA)

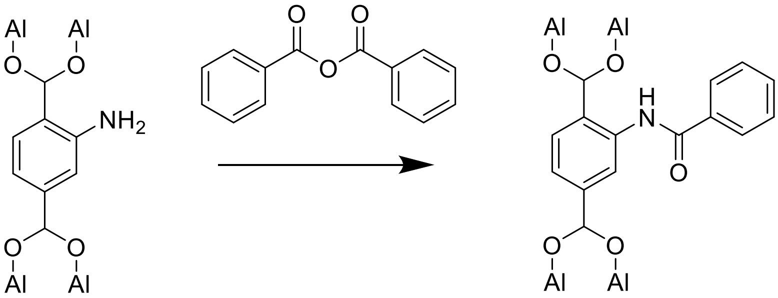

Before Irradiation	After Irradiation	Infrared camera image
		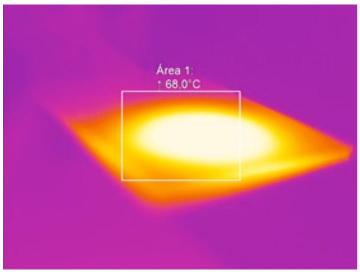

Figure S22. Photos of the formation of (MIL-101-(Al)-BA)$_3$ upon UV-Vis irradiation (265 mW·cm^{-2}) of MIL-101-NH_2-(Al) and BA: before (left), after (middle) and infrared camera image during irradiation(right).

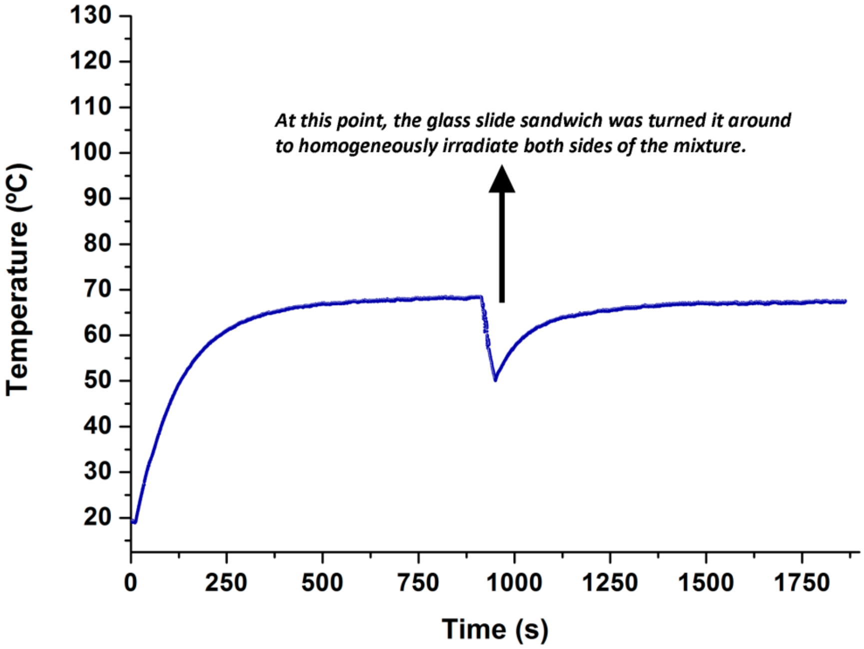

At this point, the glass slide sandwich was turned it around to homogeneously irradiate both sides of the mixture.

Figure S23. Photothermal plot of the formation of (MIL-101-(Al)-BA)$_3$ upon UV-Vis irradiation of MIL-101-NH_2-(Al) and BA at 265 mW·cm^{-2}.

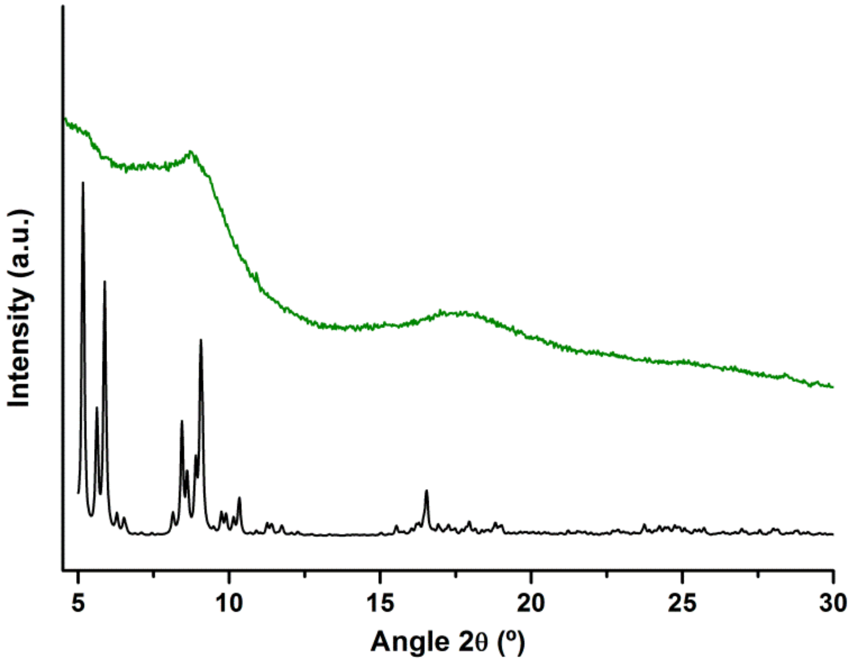

Figure S24. XRPD patterns for simulated MIL-101-NH_2-(Al) (black) and synthesised (MIL-101-(Al)-BA$)_3$ (green) upon UV-Vis irradiation at 500 mW·cm^{-2} for 30 min.

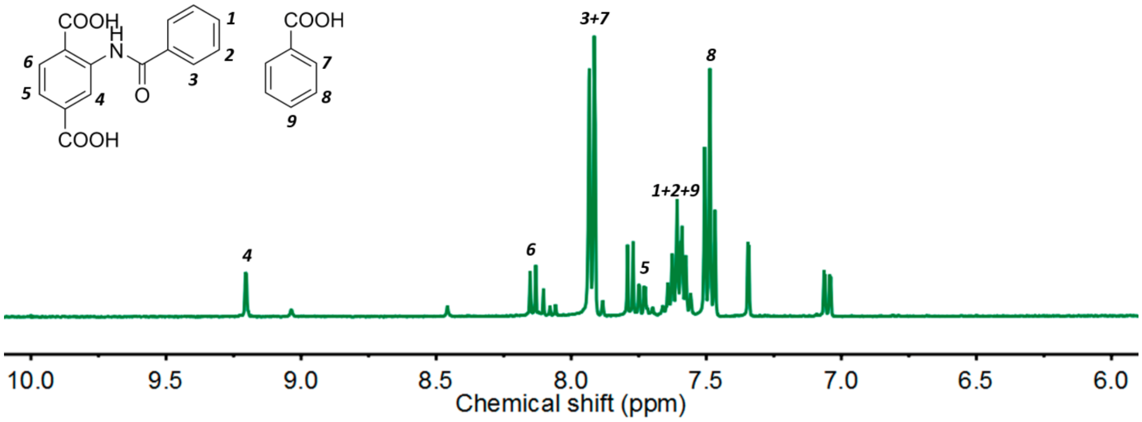

Figure S25. ^{1}H NMR spectrum of digested (MIL-101-(Al)-BA$)_3$ upon irradiation at 500 mW·cm^{-2} (light guide-to-sample distance: 7 cm. NMR solvent: DMSO-d_6/HF.

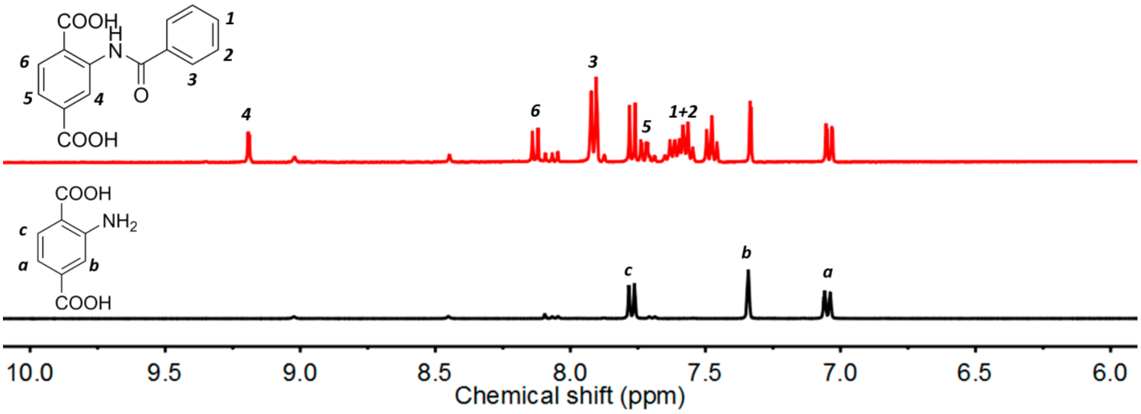

Figure S26. ^{1}H NMR spectrum of digested (MIL-101-(Al)-BA)$_3$ (red) upon irradiation at 265 mW·cm^{-2} (light guide-to-sample distance: 9 cm), as compared to that of activated MIL-101-NH$_2$-(Al) (black). NMR solvent: DMSO-d_6/HF.

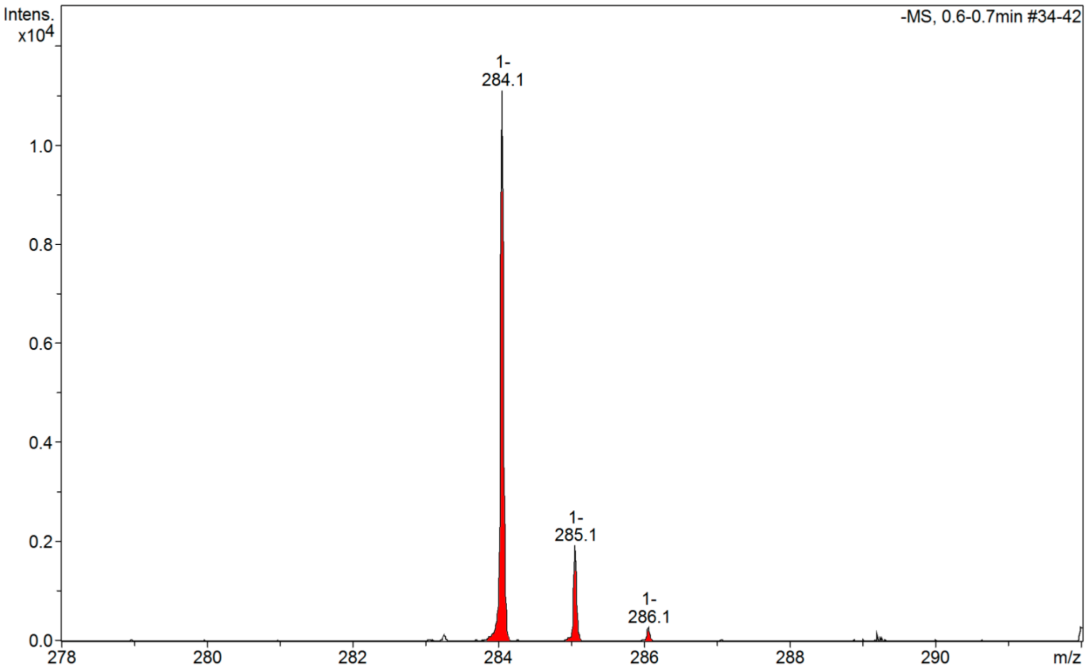

Figure S27. ESI-MS spectrum of digested (MIL-101-(Al)-BA)$_3$.

CPSM of UiO-66-NH_2 with 4-bromobenzaldehyde

Synthesis of 4-bromobenzoic acid from 4-bromobenzaldehyde

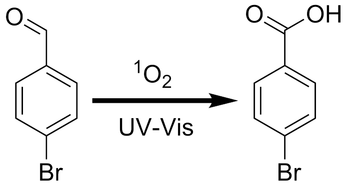

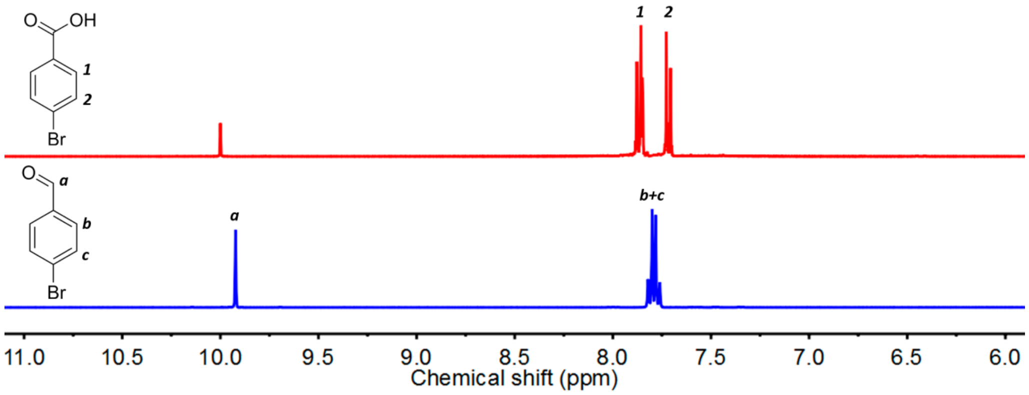

Figure S28. ^{1}H NMR spectrum of 4-bromobenzoic acid (red) upon irradiation at 500 mW·cm^{-2} (light guide-to-sample distance: 7 cm), as compared to the initial 4-bromobenzaldehyde, proving that 4-bromobenzaldehyde can be oxidized to 4-bromobenzoic acid using UV-Vis light (first step of the cascade reaction). NMR solvent: DMSO-d_6.

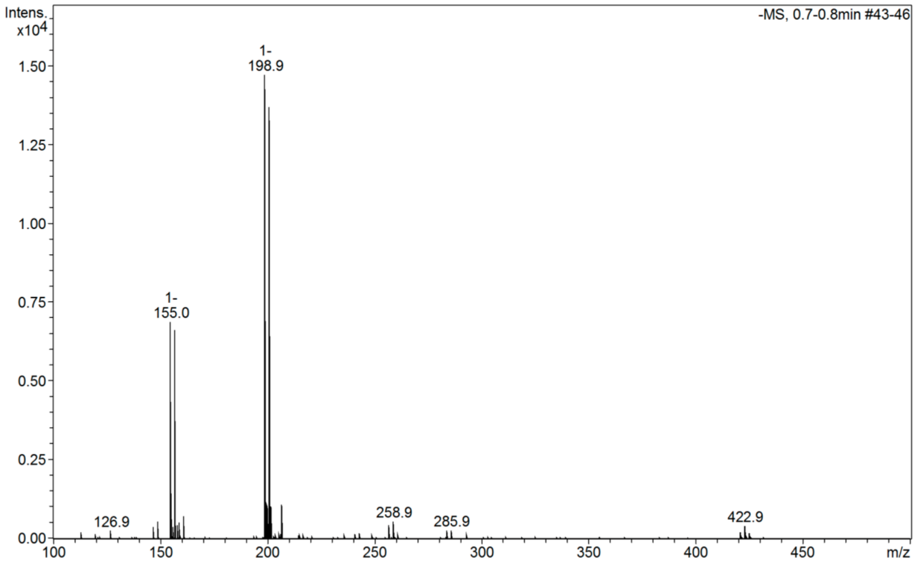

Figure S29. ESI-MS spectrum of the solid collected after irradiation of 4-bromobenzaldehyde, confirming the formation of 4-bromobenzoic acid.

CPSM reaction of UiO-66-NH_2 and 4-bromobenzaldehyde through a photoinduced cascade reaction

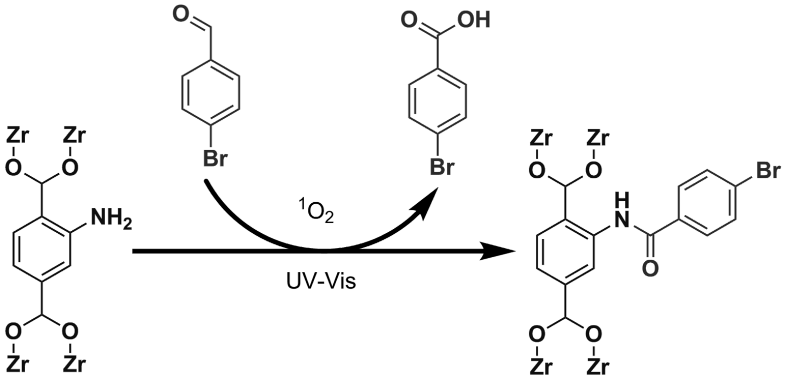

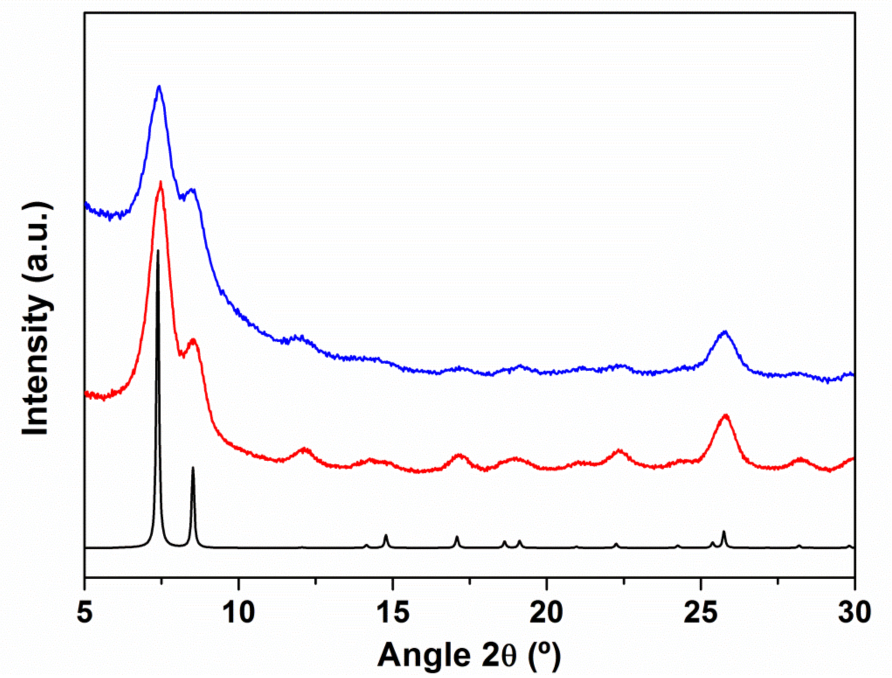

Figure S30. XRPD patterns for synthesised (UiO-66-BrBA)$_6$ (blue), activated UiO-66-NH_2 (red) and simulated UiO-66-NH_2 (black).

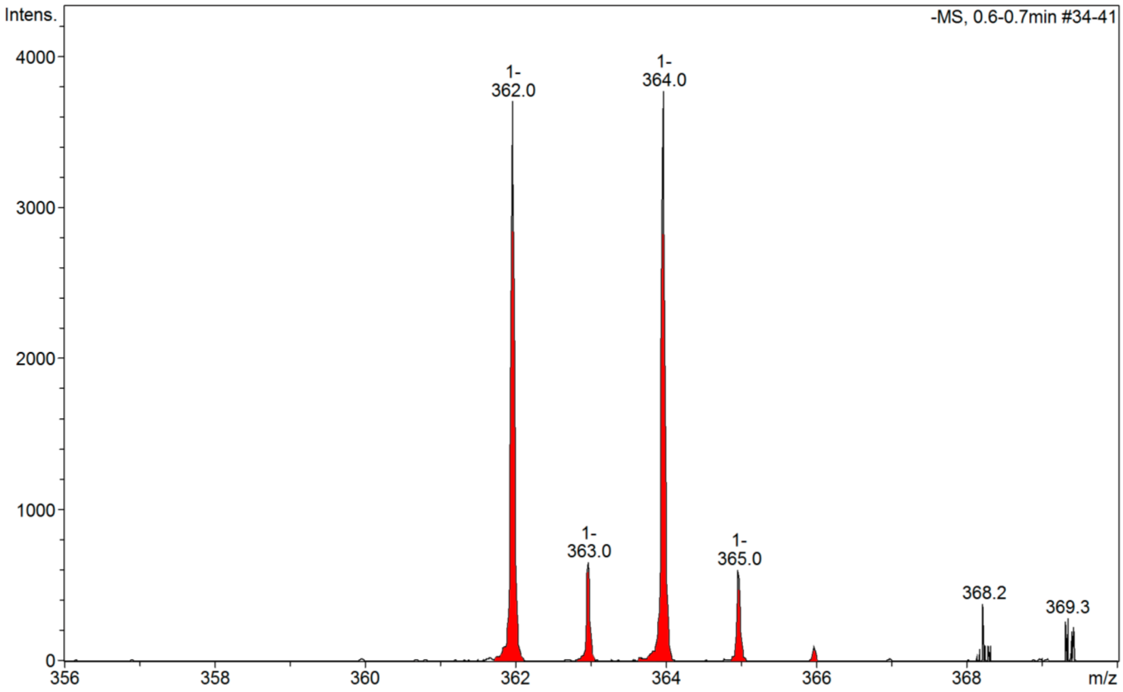

Figure S31. ESI-MS spectrum of digested (UiO-66-BrBA)$_3$.

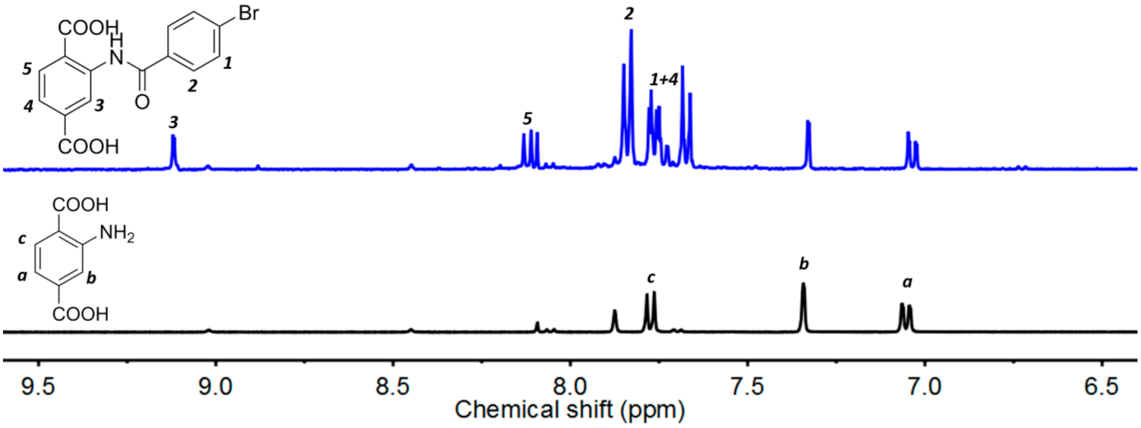

Figure S32. ^{1}H NMR spectrum of digested (UiO-66-BrBA)$_6$ (blue) upon irradiation at 500 mW·cm^{-2} (light guide-to-sample distance: 7 cm), as compared to that of activated UiO-66-NH$_2$ (black). NMR solvent: DMSO-d_6/HF.